THE INTERACTION OF OXYGEN WITH THE Mo (100) AND Mo (111) SINGLE-CRYSTAL SURFACES: CHEMISORPTION AND OXIDATION AT HIGH TEMPERATURES

Zhang, C.
Hove, M.A. Van
Somorjai, G.A.

1984-06-01

LBL-17818
Preprint

Lawrence Berkeley Laboratory
UNIVERSITY OF CALIFORNIA

Materials & Molecular Research Division

Submitted to Surface Science

THE INTERACTION OF OXYGEN WITH THE Mo(100) AND Mo(111) SINGLE-CRYSTAL SURFACES: CHEMISORPTION AND OXIDATION AT HIGH TEMPERATURES

C. Zhang, M.A. Van Hove, and G.A. Somorjai

June 1984

Prepared for the U.S. Department of Energy under Contract DE-AC03-76SF00098

LBL #17818

THE INTERACTION OF OXYGEN WITH THE Mo(100) and Mo(111) SINGLE-CRYSTAL SURFACES: CHEMISORPTION AND OXIDATION AT HIGH TEMPERATURES

C. Zhang, M. A. Van Hove and G. A. Somorjai

Materials and Molecular Research Division,
Lawrence Berkeley Laboratory and
Department of Chemistry
University of California
Berkeley, California 94720, USA

THE INTERACTION OF OXYGEN WITH THE Mo(100) and Mo(111) SINGLE-CRYSTAL SURFACES: CHEMISORPTION AND OXIDATION AT HIGH TEMPERATURES

by C. Zhang*, M. A. Van Hove and G. A. Somorjai

Materials and Molecular Research Division,
Lawrence Berkeley Laboratory
and
Department of Chemistry,
University of California, Berkeley, CA 94720 USA

ABSTRACT

The interaction of oxygen with Mo(100) and Mo(111) surfaces was studied by Auger Electron Spectroscopy, Low-Energy Electron Diffraction and Thermal Desorption Spectroscopy over a wide range of oxygen pressure (1×10^{-8} - 5×10^{-5} Torr), temperature (823K - 1200K) and exposure (0.1 - 10,000 L). With increasing oxygen exposure on Mo(100), the chemisorption structures p(1x1), c(4x4), p(2x1), ($\sqrt{5}\times\sqrt{5}$) R26°33', p(2x1), p(4x1) c(2x2), p(2x1), are detected and followed by the formation of (110) and (112) facets. On Mo(111), the (4x4) and (1x3) surface structures are detected and followed by the formation of (112) facets with (2x1) and then (3x1) superlattices. For exposures exceeding ~2000 Langmuir, an oxide grows on the facets. On Mo(100), the oxide formed from 823 to 1050K contains domains of MoO_2(110) surface parallel to the Mo(100) plane, while from 1050 to 1150K the MoO_2(110) domains are tilted ~5° away from the Mo(100) surface. On Mo(111), the oxide contains domains of MoO_2(100) surface tilted by 19.5° away from the Mo(111) surface, i.e. parallel to Mo(112) facets. The AES results show metal oxidation states corresponding to (presumably disordered) MoO_3 and an intermediate oxide, in addition to MoO_2. The higher-valence oxide seems to be stable compound on the oxide surface.

*Permanent address: Shanghai Institute of Metallurgy, Academy of Sciences of China, Shanghai, China 200050.

1. INTRODUCTION

Molybdenum is an important alloying metal that is utilized in many technologies requiring high temperatures. For this reason its initial stages of oxidation have in the past been investigated by surface science techniques (1-12) although most of these studies were restricted to the Mo(100) single crystal surface (1,3,6,7,8,12). Molybdenum oxide is an excellent catalyst for the partial oxidation of organic molecules, most notably methanol to formaldehyde (13). MoO_3, a layer compound of orthorhombic symmetry structure, has also been the subject of surface science studies for this reason (13-15). The purpose of our studies is to explore the formation of oxide films, their atomic structure and composition, starting with the metal single crystal surface from the initial stages of oxygen chemisorption to the nucleation and precipitation of the oxides. It has been established that the oxidation states of the transition metal ions and the oxygen vacancy structures around them at the surface exert a dominant influence on the selectivity of catalyzed oxidation processes (16).

We have explored oxygen chemisorption and oxide formation starting with the clean (100) and (111) crystal faces of molybdenum in the temperature range of 900 - 1200K and in the oxygen pressure range of 10^{-8} - 10^{-5} Torr. The changing surface structures were monitored by low energy electron diffraction (LEED) while the variations of surface composition and metal oxidation states were measured by Auger electron spectroscopy (AES) peak ratios and peak shapes. Thermal desorption was used to determine oxygen heats of adsorption on the metal surface.

We found oxygen chemisorption structures on the Mo(100) crystal face that were identical to those reported by Ko and Madix (7) and Bauer and Poppa(3).

On the Mo(111) surface, which has not been much explored previously, we observe, with increasing oxygen exposure, (4x4) and (1x3) chemisorption structures, followed by Mo(112) facets with (1x2) and (1x3) superlattices. At higher exposures, oxides are found to grow on the facets of both Mo(100) and Mo(111) surfaces. Ordered structures appear on the facets, which can be identified as surfaces of the monoclinic MoO_2 oxide phase. In addition, the presence of MoO_3 and intermediate oxides is also detected.

2. EXPERIMENTAL

All experiments were carried out in a stainless steel ultra-high vacuum system with base pressure of $\sim 1 \times 10^{-10}$ Torr. The samples of Mo(100) and Mo(111), cut from a 99.9% pure molybdenum single crystal rod of ~6mm diameter, were oriented and polished within ±0.5° of the nominal plane.

The AES and LEED studies were performed with four-grid Varian LEED optics. To prevent sample damage, the AES beam energy an current density were as low as possible: 1.5kV and $\sim 10^{-5}$ A/cm^2 respectively. Other AES parameters were: modulation voltage: 4V; time constant: 0.3 sec; and scanning speed: 100V/min.

Thermal desorption spectroscopy (TDS) was carried out with a UTI mass spectrometer. The sample was heated resistively at a rate of 50 deg/sec, the temperature being measured by a W(5%Re)/W(26%Re) thermocouple.

The crystal surfaces were cleaned by heating to 2000K under 1×10^{-6} Torr oxygen for 0.5 to 2 hrs, depending on the initial carbon concentration, until no carbon could be detected by AES. Then the samples were annealed in UHV for a few minutes to remove the residual oxygen from the surface.

Ion sputtering was carried out using ~5×10^{-5} Torr argon with 1.5kV beam energy.

The surface oxygen concentration was calibrated using two different coverages of dissociated CO(β) states on Mo(100) (17,18). One coverage corresponds to a saturated CO(β) state with a sharp (1x1) LEED pattern and an Auger peak ratio $O_{(512)}/Mo_{(221)} = 0.08$; the other corresponds to a half saturated CO(β) state with a c(2x2) LEED pattern and an Auger peak ratio $O_{(512)}/Mo_{(221)} = 0.04$. The AES ratio $O_{(512)}/Mo_{(221)}$ for one monolayer of atomic oxygen on Mo(100) is 0.16.

3. RESULTS AND DISCUSSION

3.1 Oxygen Chemisorption and Oxidation on the Mo(100) Surface

It is necessary to be able to distinguish between the presence of clean Mo, of chemisorbed oxygen on Mo and of the oxides MoO_2 and MoO_3. We find that the molybdenum $M_{45}NN$ Auger transitions allow these surface phases to be identified. The oxide MoO_3 produces substantial spectral differences for these transitions, compared to the other phases. But the differences are relatively small, though detectable and reproducible, upon oxygen chemisorption on the clean surface and upon MoO_2 formation. The distinction between clean Mo, chemisorbed oxygen on Mo and the MoO_2 phase is therefore aided in our experiments by the observation of LEED patterns and TD spectra.

AES Measurements

Auger spectra measured for $M_{45}NN$ transitions in Mo(100) are presented in Figure 1 at various exposures to oxygen. The spectra were essentially identical after heating to 923, 1050 and 1200K.

Deposition of oxygen on Mo(100) in the exposure range up to about 1000L (not shown in Fig. 1) produces very small effects (peak shifts and broadenings) in the Auger spectra in the $M_{45}NN$ region of molybdenum, suggesting chemisorption rather than oxidation. Between about 1000L and about 5000L, the Auger spectra change markedly, which we ascribe to MoO_3 and intermediate oxide formation (2): $M_{45}VV$ peak splitting, new peak at 178eV, $M_{45}N_{23}$ and $M_{45}N_1N_{23}$ peak shifts, Fig. 1. Above 5000L, no noticeable changes occur in the Auger spectra. The exact exposures between which oxidation occurs depend to some extent on both the oxidation temperature and the oxygen pressure: a lower oxidation temperature and a higher oxygen pressure lower the required exposure at which the oxidation starts and the exposure at which it is completed. However, the final Auger spectra of the oxygen-saturated oxide surface do not depend on the oxidation temperature.

We have measured the Auger peak height ratio $O_{(512)}/Mo_{(221)}$ as a function of oxygen exposure as shown in Figure 2. These results exhibit four behavior regimes. The ratio first increases steadily in the chemisorption phase up to 1.5L, then increases very slowly during a phase interpreted as facetting (see below); it increases again during bulk oxidation about 1000L, saturating when the oxidation is complete near 5000L.

LEED Patterns

Many different ordered LEED patterns are observed on Mo(100) as a function of oxygen exposure. These are listed in Table 1 as a function of coverage, which was calibrated as 0.5 monolayers for the first p(2x1) structure. The pattern sequence is p(1x1), c(4x4), p(2x1), ($\sqrt{5}$x$\sqrt{5}$)

R26°33', p(2x1), p(4x1), c(2x2) and p(2x1) for exposures up to 1.5L. These chemisorption structures are similar to those reported previously (3,7), as Table 1 indicates.

Above 1.5L exposure, the LEED patterns show the development of both (110) and (211) facets. During this process the Auger spectra are not modified: we interpret this as chemisorption on top of the facets rather than oxidation. With increased exposure, the LEED patterns become less sharp, indicating breakup of the facets and disordered oxygen adsorption on the facets.

At exposures above ~1000L, the LEED pattern is gradually modified in a temperature-dependent fashion, cf. Figure 3, while the Auger spectra indicate that bulk oxidation takes place. The new patterns are stable under any further oxygen exposure. The pattern obtained at 1050K under 3×10^{-5} Torr O_2 (Fig. 3) can be interpreted as due to domains of MoO_2(110), i.e. (110) faces of MoO_2 crystallites, where the MoO_2(110) plane is parallel to the Mo(100) plane: four domain orientations, allowed by the Mo(100) surface symmetry, explain the observed pattern. The epitaxy is such that the [100] or [001] or [101] directions of the MoO_2 crystal are parallel to the [010] and [001] directions of the Mo crystal.

The pattern obtained at higher temperatures (1150-1200K) under the same pressure of 3×10^{-5} Torr O_2 (Fig. 4a,b), on the other hand, is somewhat different. It can be interpreted as due to facets of MoO_2(110) surface tilted by about 5° with respect to the Mo(100) surface in four azimuths rotated 90° from each other. Quantitative interpretation of this pattern yields an oxide unit cell with sides of 5.5 ± 0.05Å and 7.25 ± 0.05Å and a subtended angle of 117 ± 5°. This is very close to the ideal

$MoO_2(110)$ surface, which has unit cell sides of 5.55Å and 7.35Å and a subtended angle of 119.5°.

Oxidation at slightly higher temperature (1220K) under 3×10^{-5} Torr O_2 for 5 minutes resulted in a rather different LEED pattern: c(4x4) without facetting (Fig. 4c). We have not been able to interpret this pattern.

Desorbing oxygen by heating the oxidized or chemisorbed oxygen covered surface to 1600K or higher in UHV shows that all the structures discussed above form reversibly.

Thermal Desorption Behavior

Heating the oxidized Mo(100) surface in UHV resulted in the following fragments observed by Thermal Desorption Spectroscopy: MoO_3(mass 146), MoO_2(130), MoO(114), Mo(98) and O(16). The peak desorption temperatures for all these fragments are mutually identical (~1400K) with the exception of oxygen which desorbs ~150K higher than the others. From the exposure dependence of the TDS peaks, we find that this is a zero-order desorption (or evaporation) process. The heat of desorption (or evaporation) is found to be 121 ± 5 kcal/mol.

Sputtering and Annealing Behavior

Upon sputtering the fully oxidized surface with Ar^+ ions for 30 min, the LEED pattern disappears and the Auger and TD spectra indicate the disappearance of the MoO_3 phase, which has been reduced to the MoO_2 phase, at least within the Auger escape depth. Subsequent annealing of this sputtered surface in UHV at 1050 to 1200K for about 1 to 2 min causes the Auger spectrum to revert to that of the initial oxide. Thus

MoO_3 has formed again (in addition to the MoO_2) (Fig. 5), presumably by oxygen diffusion to the surface. This also shows that MoO_3 is stable in the sense that no excess oxygen is needed to produce MoO_3.

3.2 Oxygen Chemisorption and Oxidation on the Mo(111) Surface

AES Measurements

The AES spectra for the Mo(111) surface during oxygen exposure at 923, 1050 and 1200K are very similar to those on Mo(100), including the oxygen exposure dependence of the AES changes. The variation of the AES O/Mo ratio during exposure of Mo(111) to oxygen is also very similar to the case of Mo(100), as shown in Fig. 6 which is to be compared with Fig. 1 for Mo(100). Thus we observe a very similar chemisorption and subsequent oxidation behavior on both Mo(100) and Mo(111).

The dip in the Auger ratio of Fig. 6 at an exposure of ~1.5L can be understood as due to the sudden onset of facetting; this increases the surface area, exposing more molybdenum, Mo, to the AES probe.

LEED Patterns

The first ordered structure formed after oxygen adsorption on the Mo(111) surface at 1050K and cooling to room temperature is a (4x4) structure, as found previously (5). It has maximum definition at 0.5L, cf. Fig. 7a. With further exposure, the background increases, the sharp (4x4) pattern weakens and a diffuse (1x3) pattern appears. At about 0.7L, the (1x3) pattern is most pronounced having completely replaced the (4x4) structure (Figure 7b). This (1x3) pattern was not observed in previous work. Then, with further oxygen exposure at 1050K, streaks appear in the pattern. When the exposure reaches about 1.5L, a facetted structure develops, which is most pronounced at about 3L (Fig. 8a). It corresponds to facets of (211) orientation, with three azimuthal orientations 120° from one another, as allowed by the substrate symmetry. Each of these facets has a (1x2) superstructure with double spacing in the less densely packed $[1\bar{1}0]$ direction and normal spacing in the $[11\bar{1}]$ direction. With further exposure, these (112)-(1x2) facets are gradually replaced by (112)-(1x3) facets which have a threefold spacing in the $[1\bar{1}0]$ direction and a normal spacing in the $[11\bar{1}]$ direction. By 8L, the (112)-(1x3) facet structure has completely replaced the (112)-(1x2) facet structure (Fig. 8b). These (112)-(1x3) facets remain on the surface for oxygen exposures up to 2000L. Above 2000L, the facet pattern becomes weaker and diffuse. Finally, no pattern remains at about 3000L. Under these conditions AES shows no oxidation, but rather chemisorption.

Heating the sample, which has been exposed to oxygen by over 1000L, to about 1200K for ~1 min, under the same oxygen pressure, ~3x10^{-5} Torr, produces some rings with threefold symmetry on the dark LEED screen. Similarly to the case of Mo(100), the ring pattern formation corresponds to the onset of changes in Auger spectra, i.e. to the start of the bulk oxidation. All the ring patterns formed at different temperatures are the same, except at the lower oxidation temperature, where the rings break up into sharper spots. All these patterns correspond to facetted structures, where the facets have (211) orientation with respect to the substrate. The sharp pattern (Fig. 8c) allows us to determine that the unit cell on the facet surface is rectangular with sides of 5.6Å and 4.8Å; this coincides with the unit cell shape and size of the MoO_2(100) surface. It appears therefore that a MoO_2 surface oxide has formed, such that its exposed (100) face takes on the Mo(211) orientations of the substrate (this corresponds to a 19.5° tilt). In the case of the ring patterns, these oxide facets have arbitrary azimuthal orientation on the (211) substrate planes. In the case of the sharper spots, the oxide facets have only a few allowed azimuthal orientations imposed by the substrate lattice, defined as the [010] direction of MoO_2 being parallel to the $[1\bar{1}0]$ direction of Mo. In this situation there is near-perfect epitaxial match between the MoO_2(100) lattice and the Mo(211) lattice: after doubling the Mo(211) period in the $[11\bar{1}]$ direction, there remain only a 4% and a 8% misfit in the two directions, respectively.

Similarly to the case of Mo(100), heating the oxidized or chemisorbed surface to 1600K or higher temperature in UHV shows that the structures form reversibly.

Thermal Desorption, Sputtering and Annealing Behavior

The results of TDS, sputtering and annealing experiments for the Mo(111) crystal face are identical to those for Mo(100), with one minor difference: the heat of desorption (or evaporation) from Mo(111) is 114 ± 5 kcal/mole rather than 121 ± 5 kcal/mole on Mo(100).

4. SUMMARY

Several ordered surface structures of chemisorbed oxygen were produced or reproduced upon exposure of the Mo(100) crystal face to oxygen in the temperature range of 823-1200K and pressure range of $1\times10^{-9} - 5\times10^{-5}$ Torr: p(1x1), c(4x4), p(2x1), ($\sqrt{5}\times\sqrt{5}$) R26°33', p(2x1), p(4x1), c(2x2) and p(2x1). Similarly, on Mo(111), we produced the structures (4x4) and (1x3). The formation of these surface structures is followed by facetting: (110) and (112) facets grow on Mo(100), while (112) facets grow on Mo(111), the latter exhibiting (2x1) and (3x1) superlattices.

For exposures exceeding ~2000L, oxides grow on these surfaces. An ordered oxide of the MoO_2 phase becomes visible in LEED. On Mo(100), MoO_2(110) surfaces show up, which can be parallel to Mo(100) (at temperatures between 823 and 1050K) or tilted by 5° with respect to the Mo(100) surface (at temperatures between 1050 and 1150K). On Mo(111), MoO_2(100) surfaces appear, tilted by 19.5° from the Mo(111) surface (ie. parallel to Mo(112) facets). In addition, AES detects the presence of MoO_3, which must be disordered. The MoO_3 oxide seems to be stable on the oxide surface.

ACKNOWLEDGEMENTS

This work was supported by the Director, Office of Energy Research, Office of Basic Energy Sciences, Materials Sciences Division of the U.S. Department of Energy under Contract Number DE-AC03-76SF00098.

One of us (C. Zhang) acknowledges financial support from the Chinese Education Ministry.

REFERENCES

1. H.M. Kennett and A.E. Lee, Surface Sci. 48, 591-605, 606-616, 617-623, 624-632, and 633-648 (1975).
2. T.T. Lin and D. Lichtman, J. Vac. Sci. Technol. 15, 1689-1694 (1978).
3. E. Bauer and H. Poppa, Surface Sci. 88, 31-64 (1979).
4. A. Benninghoven, O. Ganschow and L. Wiedmann, J. Vac. Sci. & Techn. 15, 506-509 (1978).
5. J. Ferrante and G.C. Barton, NASA TN D-4735.
6. H.M. Kennett, A.E. Lee, J.M. Wilson, Proc. Roy. Soc. Lond. A 331, 429-443 (1972).
7. E.I. Ko and R.J. Madix, Surface Sci., 109, 221-238 (1981).
8. H.K.A. Kan and S. Feuerstein, J. of Chem. Phys. 50, 3618-3623 (1969).
9. R.M. Lambert, J.W. Linnett, and J.A. Schwarz, Surface 26, 572-586 (1971).
10. E. Bauer and H. Poppa, Surface Sci. 127, 243-254 (1983).
11. M.P. Hooker and J.T. Grant, J. Vac. Sci. Technol. 12, 325-328 (1975).
12. K. Hayek, H.E. Farnsworth and R.L. Park, Surface Sci. 10, 429-445, (1968).
13. L.E. Firment and A. Ferretti, Surface Sci. 129, 155-176 (1983).
14. J. Ziokkowsk, J. of Catalysis 80, 263-273 (1983).
15. R. Erre, H. Van Damme and J.J. Fripiat, Surface Sci. 127, 48-68 and 69-82 (1983).
16. J.L. Callahan, R.K. Grasselli, E.C. Milberger and H.A. Strecker, Ind. Eng. Chem. Prod. Res. Devel. 9, 134-142 (1970).
17. T.E. Felter and P.J. Estrup, Surface Sci. 54, 179-182 (1976).
18. C. Guillot, R.Riwan and J. Le Cante, Surface Sci. 59, 581-592 (1976).

FIGURE CAPTIONS

Fig. 1: The $M_{4,5}NN$ Auger spectrum of Mo(100) during oxidation at 1200K: (a) clean surface, (b) after an oxygen exposure of 1800L, (c) of 3600L, (d) of 5400L, (e) of 45000L.

Fig. 2: The Auger peak ratio $O_{(512)}/Mo_{(221)}$ as a function of oxygen exposure during chemisorption and oxidation on Mo(100) at high temperatures.

Fig. 3: LEED patterns of the oxide formed on Mo(100) at 1050K with an oxygen exposure of 9600L: (a) electron energy of 50eV, (b) 80eV. The right-hand panels identify and relate the spots visible in the patterns.

Fig. 4: LEED patterns of the oxide formed on Mo(100) at peak 1200K (a,b) and 1220K (c): (a) 9000L (42eV) (b) 18000L (42eV) (c) 18000L (47eV); in (a) the four spots marked ⊗ correspond to the facets (110) and (112).

Fig. 5: The $M_{4,5}NN$ Auger spectrum of Mo(100) during oxidation at 1050K (a), ion sputtering (b,c,d,) and then annealing in ultra-high vacuum at different temperatures (e,f,g): (a) after 12000L oxygen exposure, (b) after ion sputtering for 8 min, (c) for 18 min, (d) for 30 min, (e) after annealing at 1050K for 2 min, (f) at 1200K for 2 min, (g) at 1400K for 1 min.

Fig. 6: The Auger peak ratio $O_{(512)}/Mo_{(221)}$ as a function of exposure during chemisorption and oxidation on Mo(111) at high temperatures. At the exposures pointed out by arrows in the low-exposure inset the corresponding LEED patterns are most pronounced.

Fig. 7: LEED patterns for chemisorbed oxygen on Mo(111) at 1050K: (a) (4x4), 0.5L, 190eV; (b) (1x3), 0.75L, 213eV.

Fig. 8: The LEED patterns of faceted structures (a,b) and the oxide (c) formed on Mo(111) at high temperatures: (a) 1050K, 3L; (b) 1050K, 8L; (c) 823K, 9000L or 1200K, 1800L.

TABLE CAPTIONS

Table 1: Comparison of chemisorption structures of oxygen on Mo(100) in the present work (a), in the work of E.I. Ko and R.J. Madix (Ref. 7) (b), and in the work of E. Bauer and H. Poppa (Ref. 10) (c). At the coverages indicated by arrows the corresponding patterns are most pronounced.

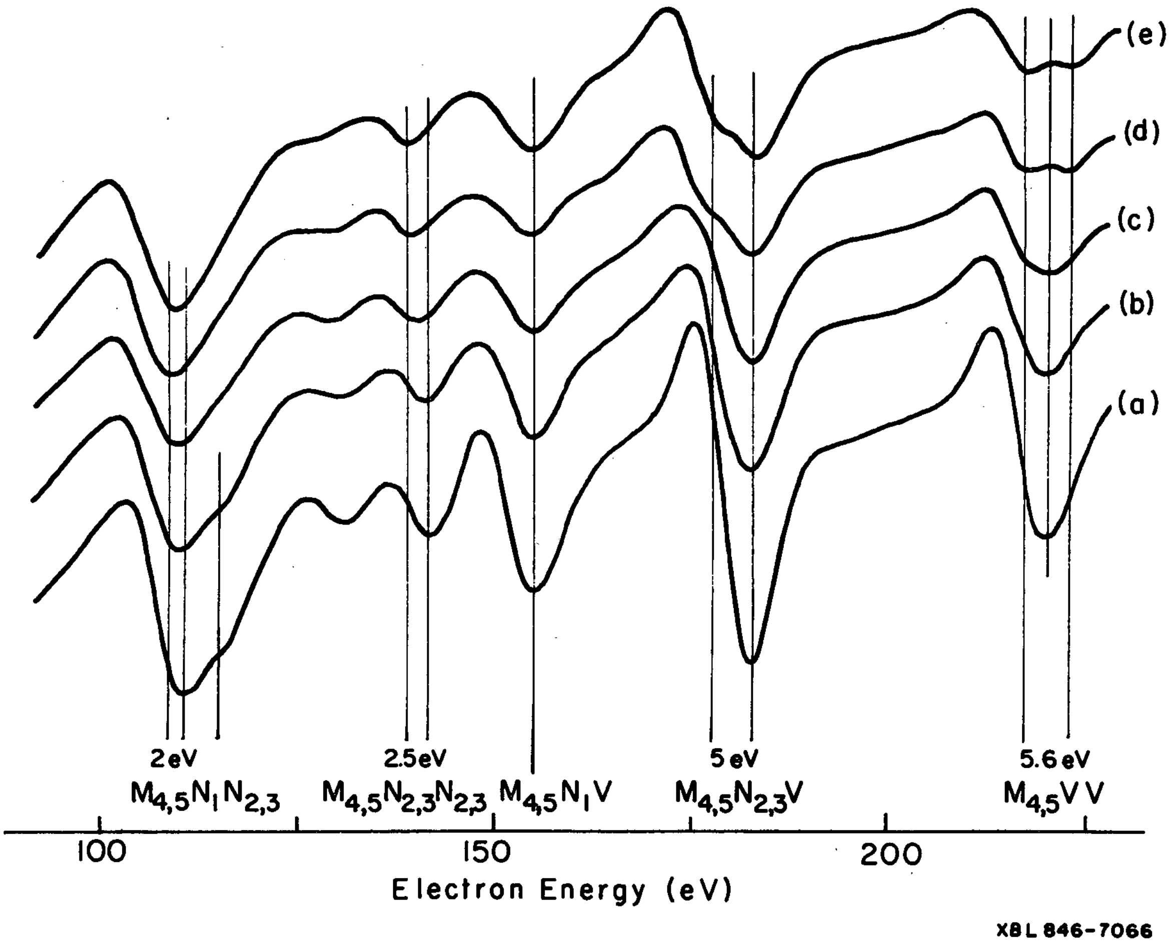
(e)
(d)
(c)
(b)
(a)
2eV
$M_{4,5}N_1N_{2,3}$
2.5eV
$M_{4,5}N_{2,3}N_{2,3}$
$M_{4,5}N_1V$
5 eV
$M_{4,5}N_{2,3}V$
5.6 eV
$M_{4,5}VV$
100
150
200
Electron Energy (eV)
XBL 846-7066

Fig. 1

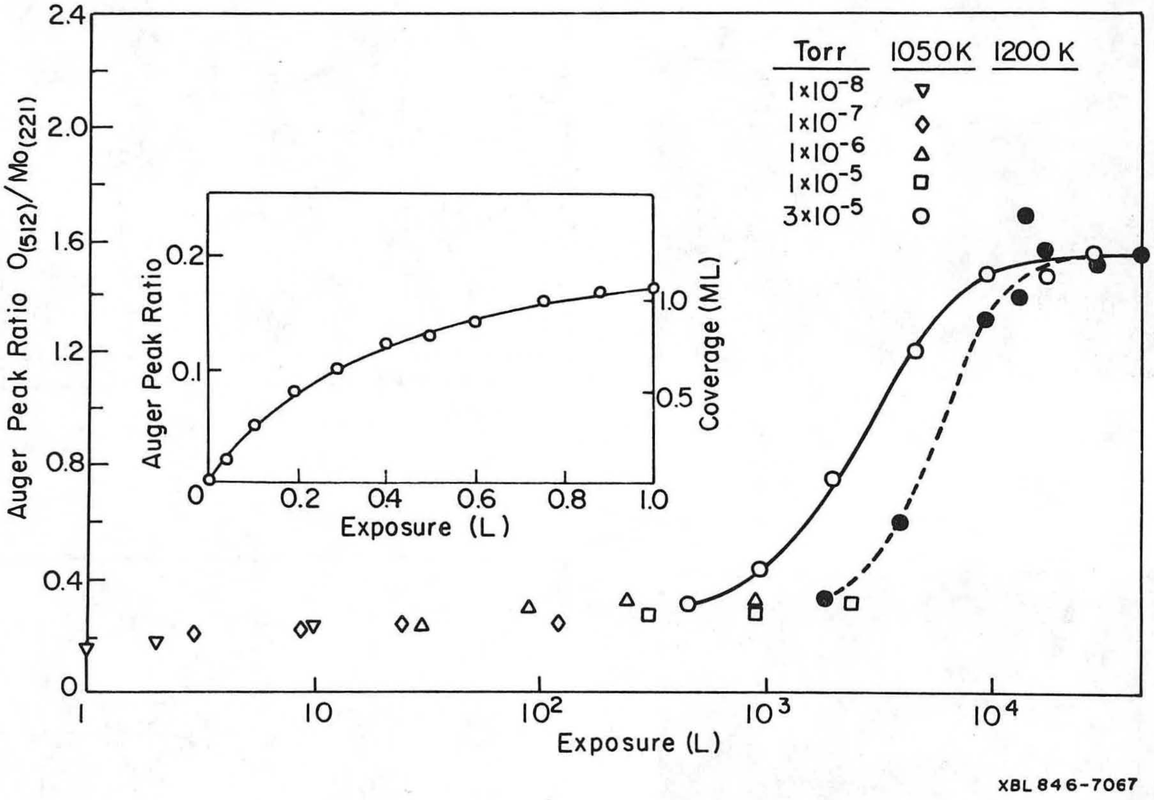
Torr
1050 K
1200 K
1×10⁻⁸ ▽
1×10⁻⁷ ◇
1×10⁻⁶ △
1×10⁻⁵ □
3×10⁻⁵ ○
Auger Peak Ratio O(512)/Mo(221)
2.4
2.0
1.6
1.2
0.8
0.4
0
1
10
10²
10³
10⁴
Exposure (L)
Auger Peak Ratio
0.2
0.1
0
0.2
0.4
0.6
0.8
1.0
Exposure (L)
Coverage (ML)
1.0
0.5
XBL 846-7067

Fig. 2

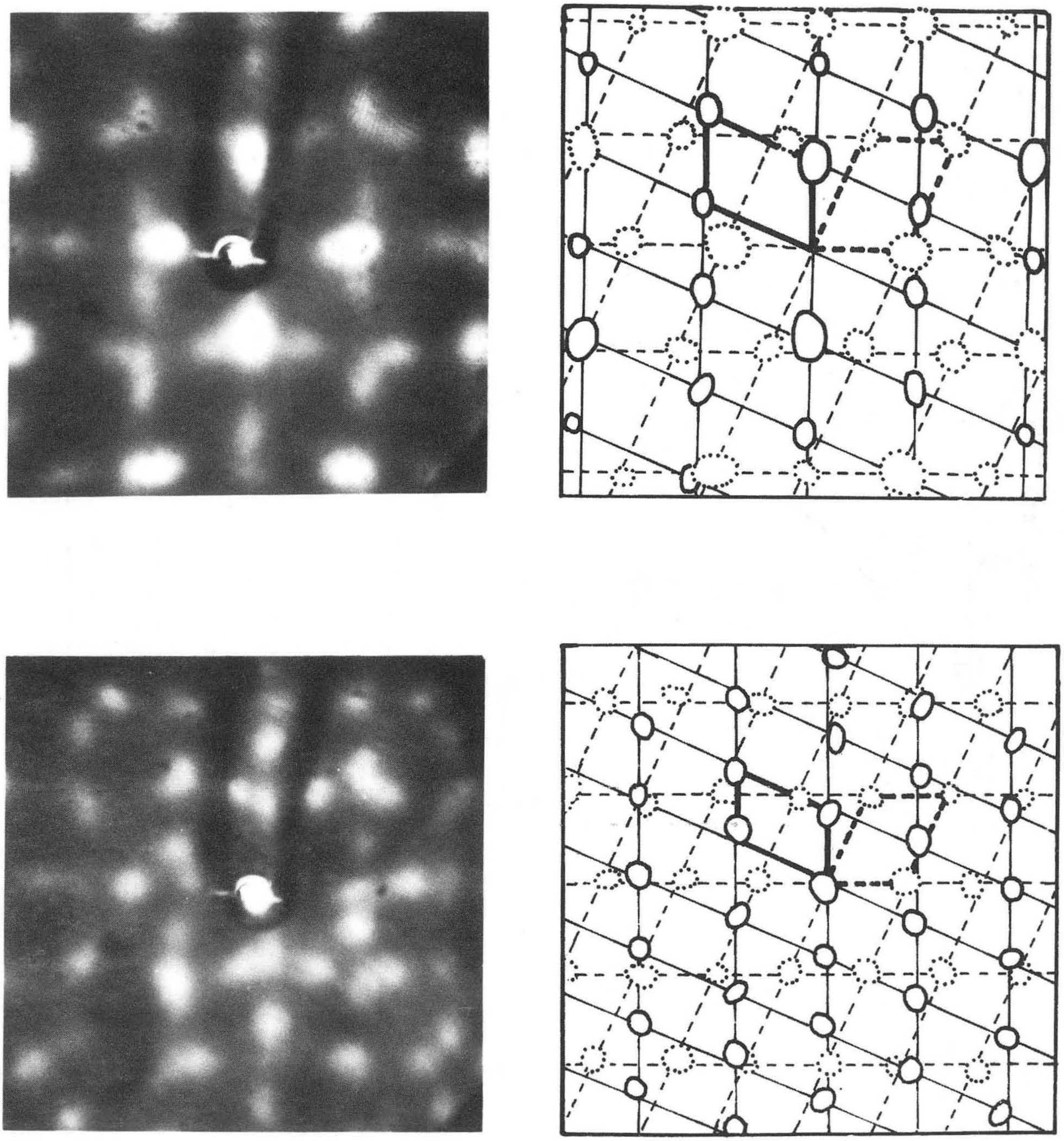

XBB 846-4537

Fig. 3

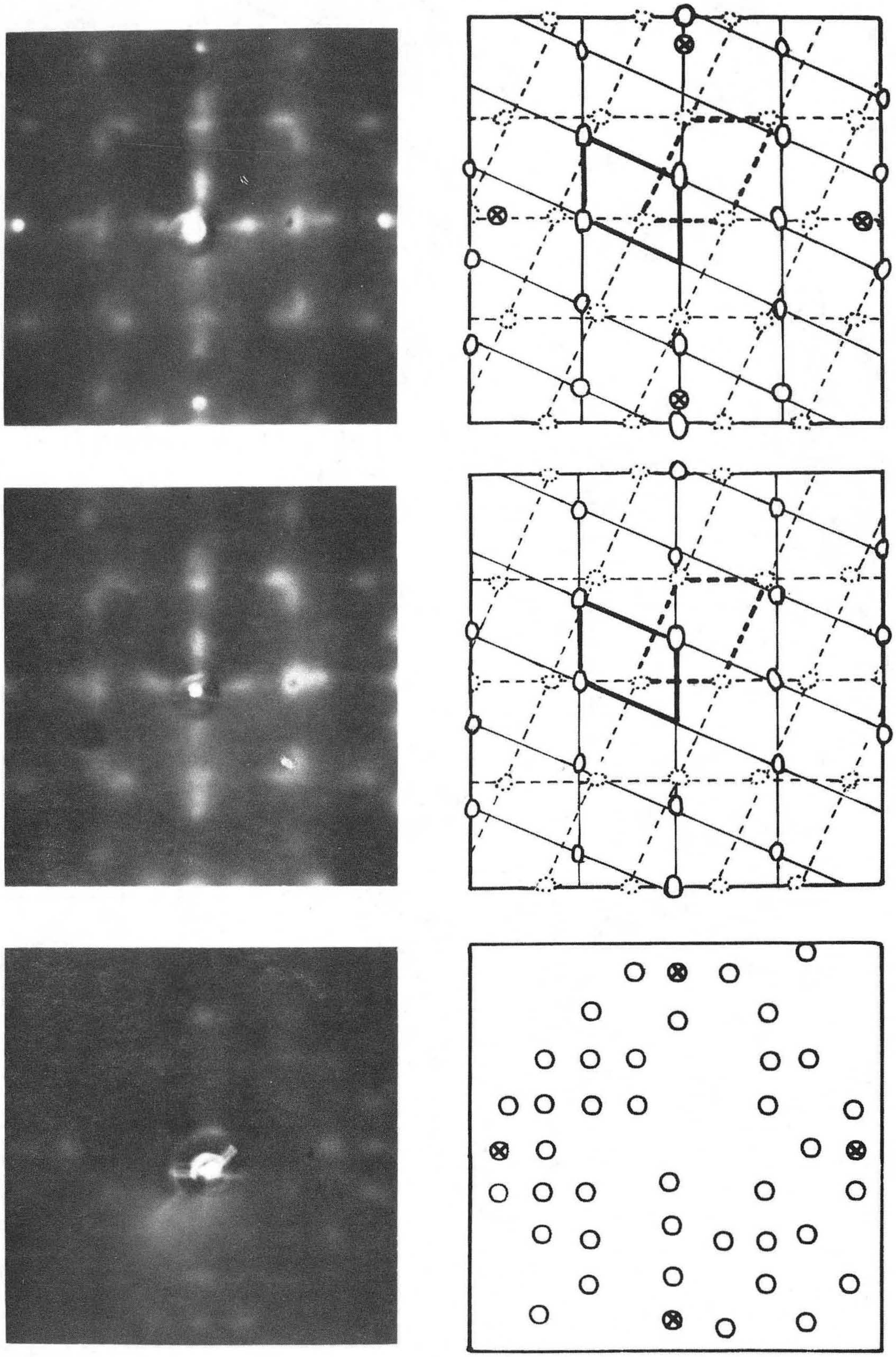

XBB 846-4538

Fig. 4

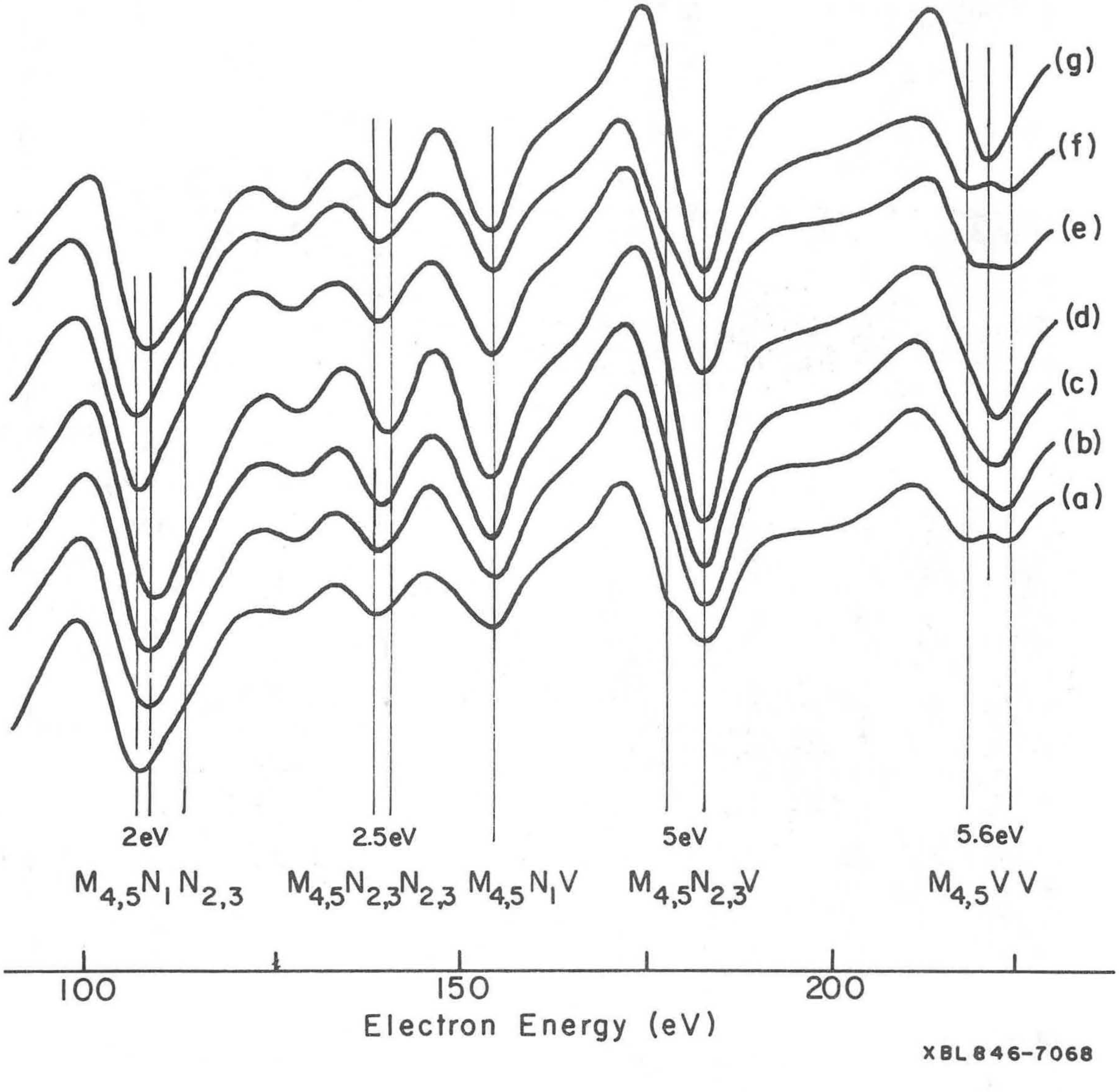
(g)
(f)
(e)
(d)
(c)
(b)
(a)
2eV
2.5eV
5eV
5.6eV
M4,5N1 N2,3
M4,5N2,3N2,3
M4,5 N1V
M4,5N2,3V
M4,5V V
100
150
200
Electron Energy (eV)
XBL 846-7068

Fig. 5

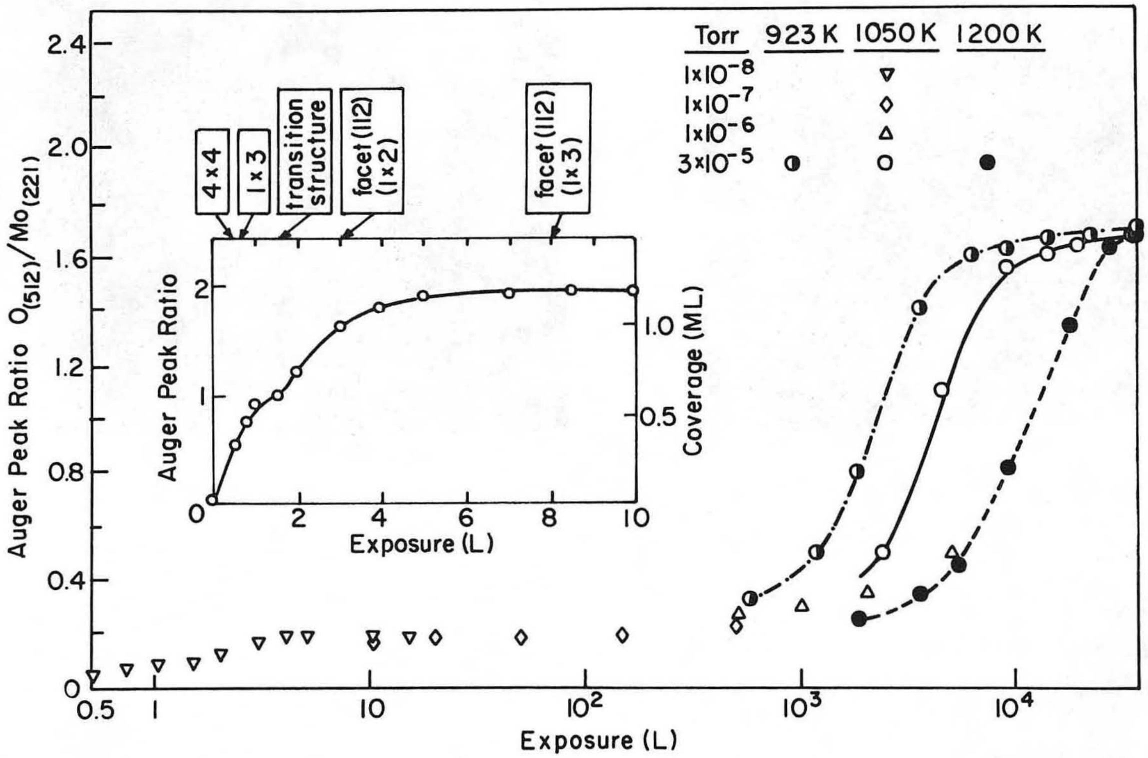

XBL846-7069

Fig. 6

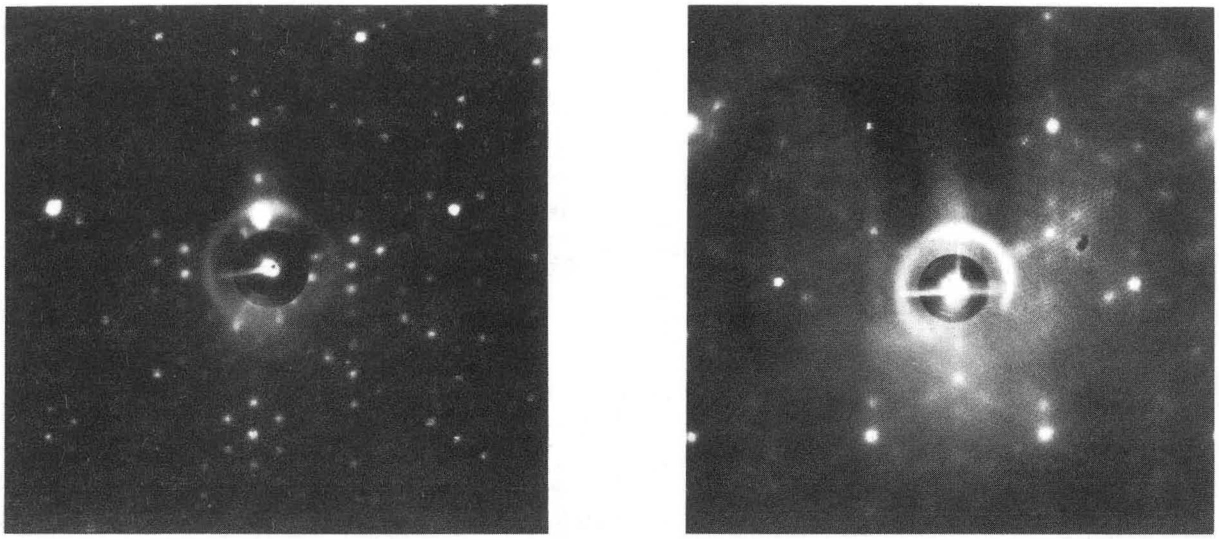

XBB 846-4536

Fig. 7

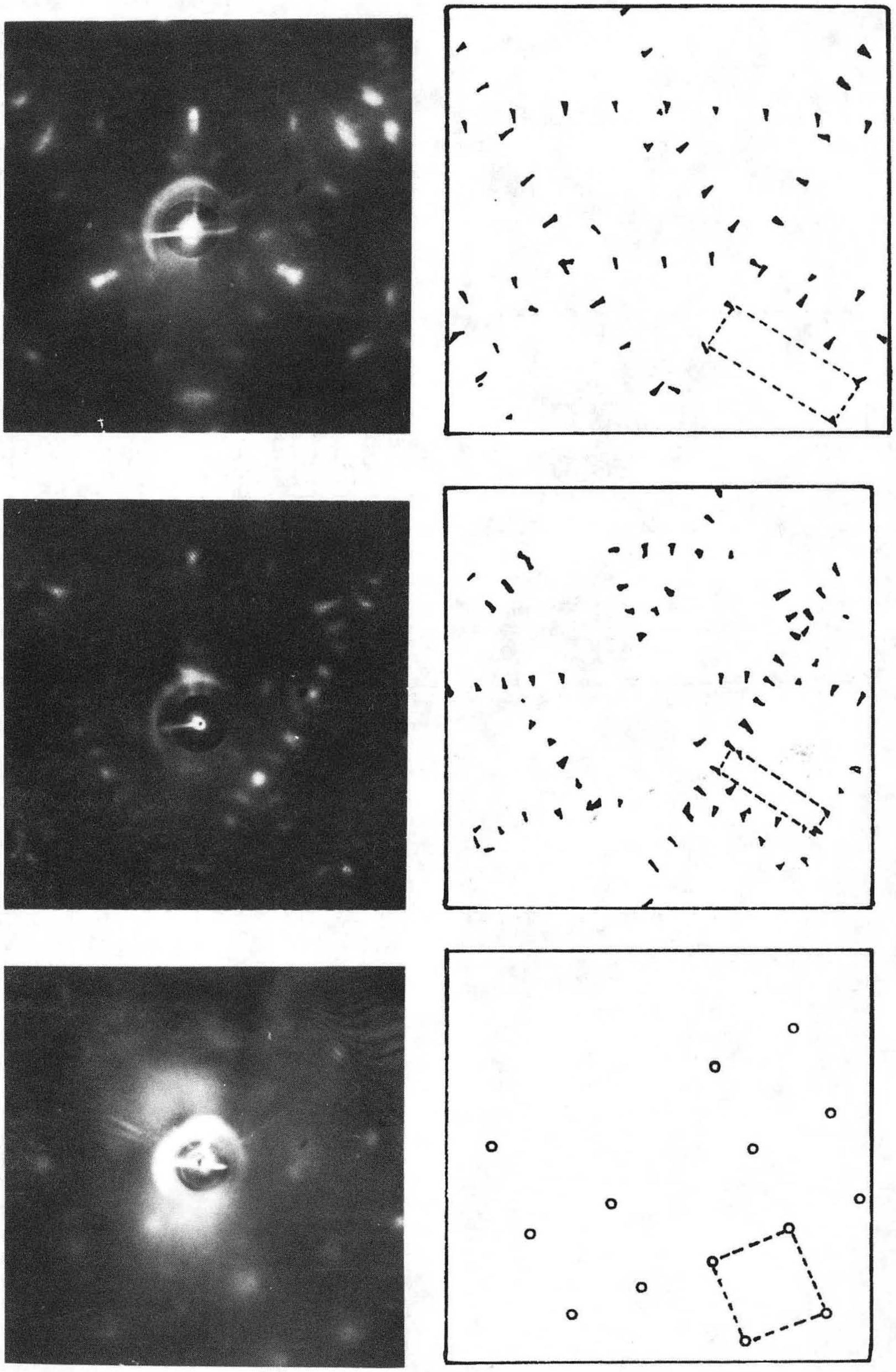

XBB 846-4539

Fig. 8

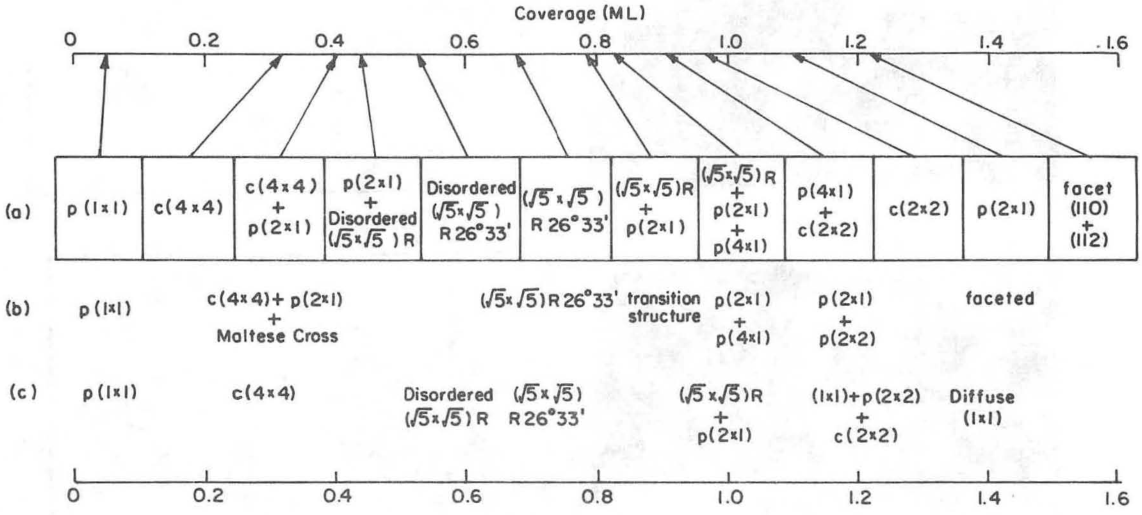

Table I

XBL 846-7070

Table 1

TECHNICAL INFORMATION DEPARTMENT
LAWRENCE BERKELEY LABORATORY
UNIVERSITY OF CALIFORNIA
BERKELEY, CALIFORNIA 94720